Vol. 3, No. 1 (2022); 1–11

Journal of Earth Sciences and Technology

http://www.htpub.org/Journal-Of-Earth-Sciences-And-Technology/

Analyzing Sensitivity of Elastic Properties on Lithology and Fluid Change, an Example from Malay Basin

Hanan Othman[a], Zaky Ahmad Riyadi[a], Maman Hermana[a]*

[a] *Universiti Teknologi PETRONAS, 32610 Seri Iskandar, Perak, Malaysia*

Article Information

Article History
Received: 07/10/2021
Accepted: 06/12/2021
Available online: 10/01/2022

Keywords
Fluid Substitution
Elastic Properties
Malay Basin
Python Code

Abstract

Understanding the sensitivity of different elastic properties towards changes in lithology and fluid type is a crucial information in hydrocarbon exploration and development. Fluid substitution was conducted on Well X in Malay Basin using the Gassmann's Equation and subsequently, the elastic property of both measured well data and fluid substitution scenarios were calculated. Cross-plots of relevant elastic property was generated to analyze the response. The best elastic property for lithology differentiation is the Poisson Ratio and Labdha-Rho/MuRho. Shear Impedance, Shear Modulus, Young Modulus and Mu-Rho are also good indicators of lithology. The elastic properties that are most sensitive towards changes in fluid type is the Lambda-Rho, Labdha-Rho/Mu0Rho, P-Impedance and Poisson Ratio. Cross-plots between Vp, density and Bulk Modulus can differentiate between oil-sand and gas-sand at 100% saturation. This understanding on the sensitivity of the elastic properties towards lithology and fluid fill will allow for future seismic-based inversion to be conducted in and surrounding this field in Malay Basin.

1. Introduction

Understanding rock properties and being able to discriminate between different lithologies and fluid fills is a crucial knowledge in the field of hydrocarbon exploration and development. A key property of a rock are its elastic properties. Elastic properties of a rock are defined by the changes (volume, length, shape, etc.) that a rock experiences as a result of stress and strain. The degree of changes is largely determined by the matrix strength (lithology) and the fluids within the pore spaces. Elastic properties are calculated and derived from compressional and shear-log data. Cross-plot analysis of elastic properties is an efficient method to differentiate between lithology and fluid fill and is also a useful input for seismic AVO inversion (Lubis, Ghosh, & Hermana, 2016).

* Corresponding author
E-mail address: maman.hermana@utp.edu.my

The fluid substitution method that is commonly conducted using Gassmann's equation is an important tool to identify and quantify fluids in a reservoir (Kumar, 2006). This method is conducted with the objective to model the changes in P-waves (Vp), S-waves (Vs) and density (ρ) for a given fluid saturation and reservoir condition (Bodunde, & Enikanselu, 2018). The information derived from this model is integral as it is capable to explain the changes in amplitude vs offset (AVO), which has become key property in analyzing the prospectivity of an area (Smith, Sondergald, & Rai, 2003). A few assumptions were made when applying the Gassman's fluid substitution. These assumptions are: 1) The background mineral matrix is isotropic in nature, 2) all contributing pore spaces are interconnected, i.e the effective porosity, 3) the shear rigidity is not affected by fluid, thus remains the same after fluid substitution (Huang et al., 2014).

Upon deriving the expected Vp, Vs and density, it is possible to calculate the elastic properties associated with the modeled condition which subsequently can be used for inversion. Changes in elastic properties due to changes in fluid type is expected as bulk modulus is highly sensitive to changes in fluid saturation (Bodunde, & Enikanselu, 2018).

In this study, we analyzed the sensitivity of the elastic parameters towards changes in lithology and fluid fill in Well X, a well from an oil field in the Malay Basin.

2. Material and Methodology

2.1 Data set and medium of calculation

The evaluation was conducted using the dataset from Well X, a well from an oil field in Malay Basin. The lithology in Well X comprises of interbedded sand and shale layers. The well information provided consisted of GR, Res, Density, Porosity, Vp, Vs, Water Saturation and Vclay Volume. The well interval is from 1519 m to 1824 m (figure 1). The sand at 1671 m is a hydrocarbon-bearing sand. All calculation and analysis were carried out in Python.

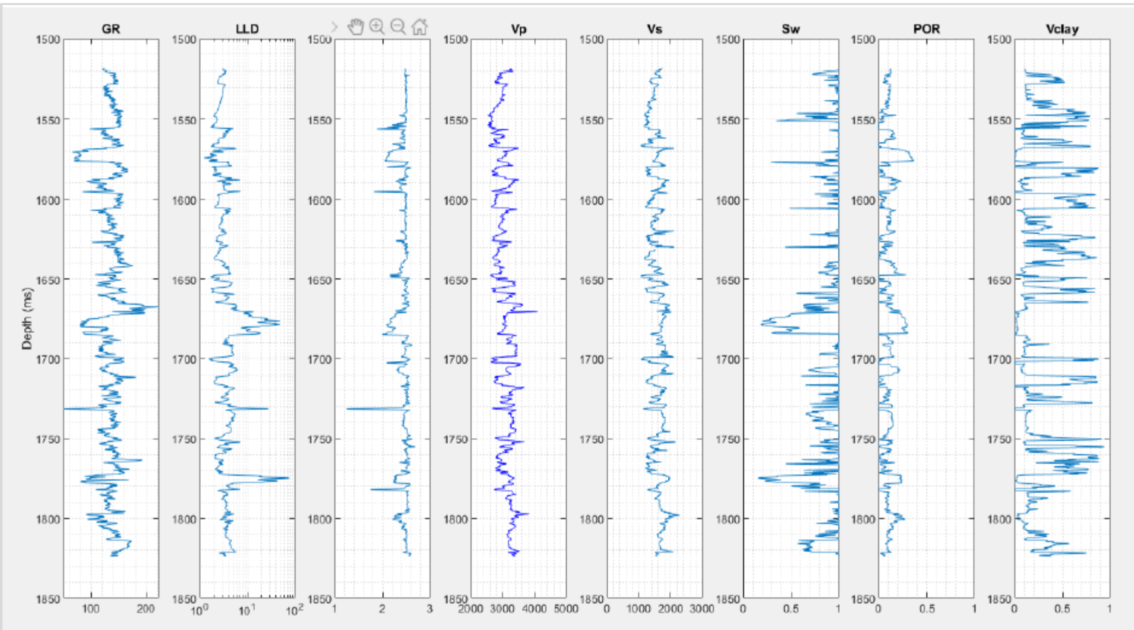

Fig. 1. Log data for interval 1519 m to1824 m from Well X, Malay Basin.

2.2 Measuring the sensitivity of elastic properties to changes in lithology

To measure the sensitivity of elastic properties to changes in lithology, the P-Impedance, Shear Impedance, Bulk Modulus, Shear Modulus, Poisson Ration were calculated using the available Vp, Vs and Density for the full well interval. The equation of each elastic properties is provided in table 1. The Python code is provided in Appendix A.1. The result was then plotted along with the other well data.

Table 1. Elastic properties equations.

Elastic Properties	Nomenclature	Equation
Compressional Velocity	V_p	V_p
Shear Velocity	V_s	V_s
P-Impedance a.k.a. Acoustic Impedance	AI	ρV_p
Shear Impedance	SI	ρV_s
Lambda-Rho	$\lambda\rho$	$(V_p\rho)^2 - 2\,(V_s\rho)^2$
Mu-Rho	$\mu\rho$	$(V_s\rho)^2$
Bulk Modulus	K	$\rho*((V_p)^2 - (4/3\,(V_s)^2))$
Shear Modulus	G	$\rho*(V_s)^2$
Young Modulus	E	$(\rho(V_s)^2 * (3(V_p)^2 - 4(V_s)^2)) / (V_p)^2 - (V_s)^2$
Poisson Ratio	σ	$((V_p)^2 - 2\,(V_s)^2) / 2((V_p)^2 - (V_s)^2)$

2.3 Measuring the sensitivity of elastic properties to changes in fluids

To measure the sensitivity of elastic properties to changes in fluid, fluid substitution was carried out using the Gassmann equation on the reservoir interval of interest which is from 1670 m to 1683 m. Fluid substitution was carried out for three scenarios which are 100% brine, 100% gas and 100% oil. The steps to calculate fluid substitution using Gassman's equation is listed in table 2. The Python code is provided in Appendix A.2.

The elastic properties were then calculated for each fluid substitution scenario as per the equation in table 1 and plotted against the well data. Cross-plots of selected elastic properties were generated to evaluate the sensitivity of respective properties to lithology and fluid change. Performing rock physics cross-plots is a recommended method for a better visualization and analysis on the rock properties (Ogbamikhumi, & Igbinigie, 2020).

3. Results and Discussion

3.1 Sensitivity of elastic properties in Well X towards changes in lithology

The calculated elastic properties for Well X were plotted along with the rest of the well data (figure 2). The ratio between Vp and Vs is a well-known indicator of lithology (Abbey, Okpogo, & Atueyi, 2017). Thus, to evaluate the sensitivity of elastic parameters to lithology, cross-plots of all elastic parameters' versus Vp/Vs was constructed with well dataset color-coded based on the Vclay value (figure 3).

Table 2. Steps to calculate Gassman Fluid Substitution

Sequence of calculation		Equations
Step 1:	Calculate Bulk Modulus (K) and Shear Modulus (G)	$K = \rho*((V_p)^2 – (4/3\ (V_s)^2))$ $G= \rho*(V_s)^2$
Step 2:	Calculate Bulk Modulus of fluid $(K_f)^1$	$K_f = (f_1/K_{f1} + f_2/K_{f2})$^-1
Step 3:	Calculate Bulk Modulus of matrix $(K_m = {}_{Kvrh})$	$K_{reuss} = (f_1/K_1 + f_2/K_2)$^-1 $K_{voigt} = (f_1K_1 + f_2K_2)$ $K_{vrh} =1/2\ (K_{voigt} + K_{reuss})$
Step 4:	Calculate Bulk Modulus of fluid $(K_f)^2$	
Step 5:	Calculate the new Bulk Modulus by applying the Gassmann's equation	$\frac{K_{sat}^{(2)}}{K_{mineral}-K_{sat}^{(2)}}-\frac{K_{fluid}^{(2)}}{\phi\left(K_{mineral}-K_{fluid}^{(2)}\right)}=\frac{K_{sat}^{(1)}}{K_{mineral}-K_{sat}^{(1)}}-\frac{K_{fluid}^{(1)}}{\phi\left(K_{mineral}-K_{fluid}^{(1)}\right)}$
Step 6:	Leave the shear modulus unchanged	$\mu_{sat}^{(2)} = \mu_{sat}^{(1)}$
Step 7:	Calculate the new bulk density due to fluid change	$\rho^{(2)} = \rho^{(1)} + \phi\ (\rho_{fluid}^{(2)} - \rho_{fluid}^{(1)})$
Step 8:	Calculate the new V_p and V_s due to fluid change	$V_p^{(2)} = ((K_{sat}^{(2)} + (4/3*\ \mu_{sat}^{(2)}))\ /\ \rho^{(2)})$^0.5 $V_s^{(2)} = (\mu_{sat}^{(2)}\ /\ \rho^{(2)})$^0.5

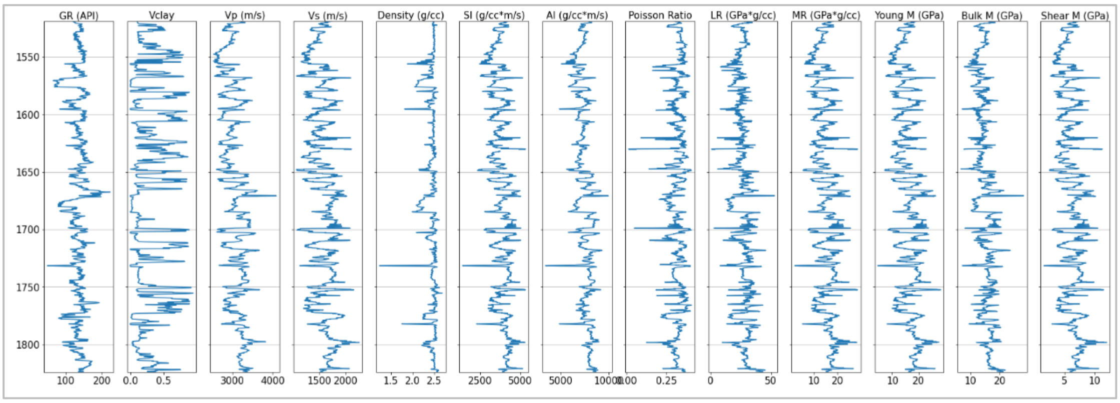

Fig. 2. Measured Well X log data and calculated elastic properties.

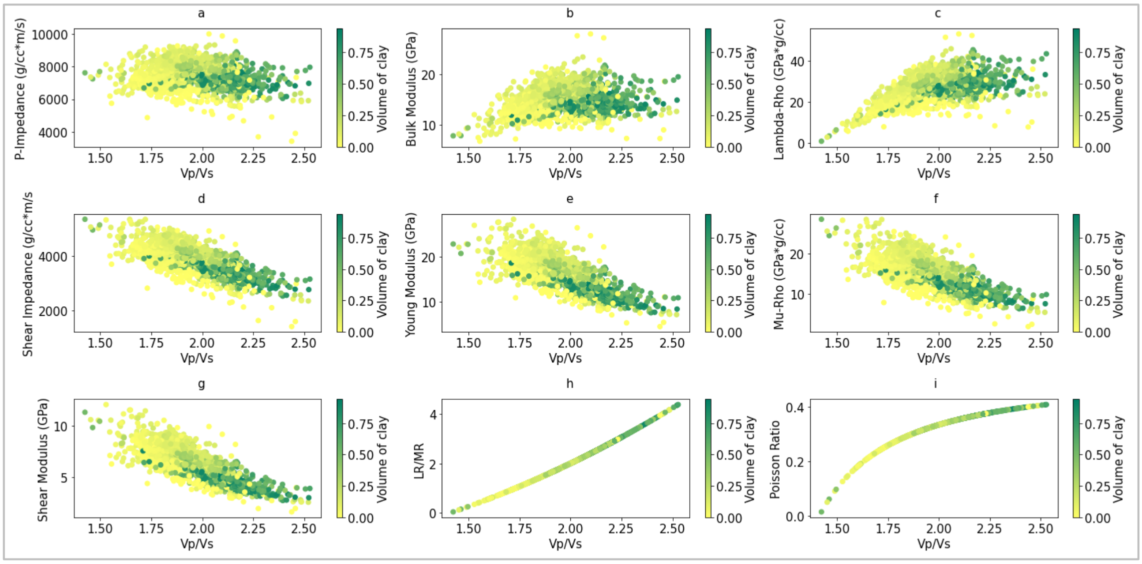

Fig. 3. Cross-plots of elastic properties of Well X against Vp/Vs.

Generally, all the cross-plots indicate some degree of sensitivity towards different lithology. This is expected because elastic properties are derived from Vp, Vs and Density whose value changes with different type of lithology. P-impedance vs Vp/Vs crossplot is relatively the least sensitive with no distinctive trend observed. This is because P-impedance only considers P-wave and density, and not S-wave.

Other elastic properties such as Shear Impedance, Shear Modulus, Young Modulus and Mu-Rho shows a much distinctive trend indicating a much higher sensitivity to lithology change. This is because these elastic properties are derived from S-wave which measures the rigidity of a rock. Sand matrix are more rigid to changes in angle compared to shale matrix. Additionally, S-waves are not affected by fluid type, thus these elastic values will remain relatively constant regardless the fluid saturation, making it a good indicator of lithology (Ogbamikhumi, & Igbinigie, 2020).

Poisson Ratio and ratio of Lambda-Rho to Mu-Rho gives the best correlation with Vp/Vs and consequently a great lithology discriminator. Both records high value for shale, while a larger range of lower values characterizes the sands.

3.2 Sensitivity of elastic properties in Well X towards changes in fluids

The calculated elastic properties for 100% brine, 100% gas and 100% oil were plotted against the measured data from Well X to evaluate the sensitivity of the elastic properties. From the plots, it is clear that the sand is a hydrocarbon-bearing sand (figure 4).

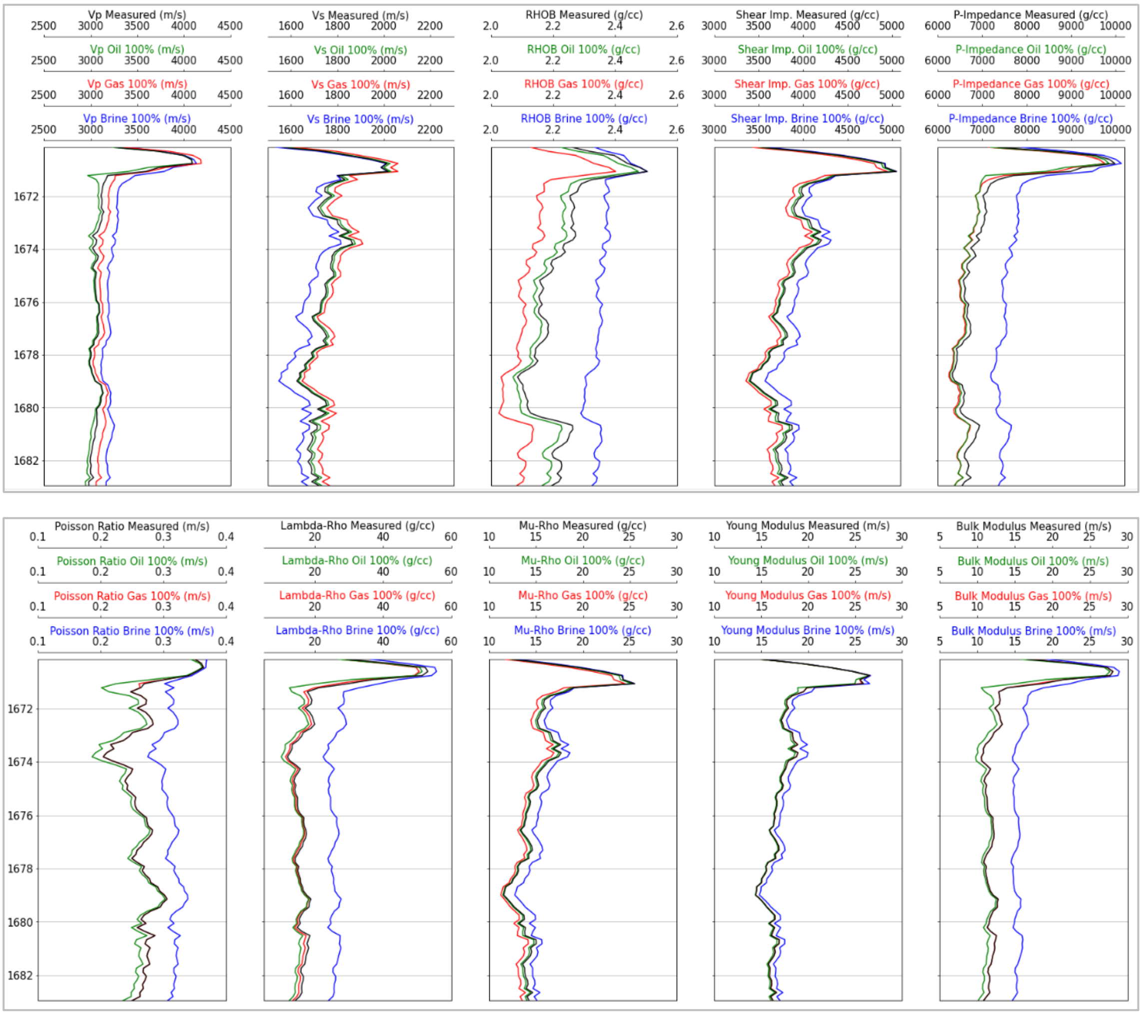

Fig. 4. Changes in elastic properties based on different fluid substitution.

From the above plot, we can clearly see that Vp, Vs and density record changes in value with different fluid fill, thus defining the changes in the elastic properties as well. P-wave and density have similar characteristics in which both records a reduction in value with the substitution of brine with hydrocarbon. Contrastingly, S-wave records an increase in value with the substitution of brine with hydrocarbon.

The plot shows that P-Impedance, Poisson Ratio, Lambda-Rho and Bulk Modulus is sensitive to fluid fill, particularly in separating between brine and hydrocarbon. However, they are less sensitive in separating between gas and oil. Mu-Rho, Shear Impedance and Young Modulus have a much lower sensitivity in fluid substitution with a smaller separation between brine and hydrocarbon.

To better visualize and analyze these sensitivities, the following cross-plots were generated (figure 5). Both measured well dataset and the calculated fluid substitution elastic parameters value were plotted together. The well dataset is color-coded based on the Vclay value, while the fluid substitution parameters are colored blue for 100% brine, red for 100% gas and green for 100% oil.

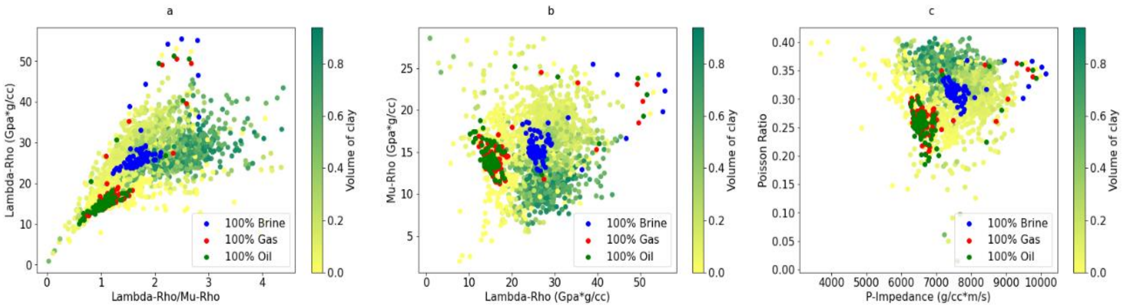

Fig. 5. Cross-plots of a) Lambda-Rho vs Lambda-Rho/Mu-Rho, b) Mu-Rho vs Lambda-Rho, c) Poisson Ratio vs P-Impedance for actual well data and fluid substitution scenario.

The cross-plot of Lambda-Rho against Lambda-Rho/Mu-Rho shows a clear distinction of both lithology and fluid fill. The shales are segregated to the far right as it records a high Lambda-Rho/Mu-Rho and moderate to high Lambda-Rho value. The brine-filled sand records a moderate value for both, while the hydrocarbon bearing sand falls to the bottom left as it records a much lower Lambda-Rho/Mu-Rho and Lambda-Rho value compared to brine-filled sands.

The cross-plot of Mu-Rho against Lambda-Rho also shows a clear separation between the brine-filled sand and the hydrocarbon-saturated sand. Lambda-Rho is able to discriminate the different fluid type with the brine-filled sand having a higher Lambda-Rho value compared to the hydrocarbon-bearing sands. However, both fluids types record the same range for Mu-Rho value, indicating that Mu-Rho is not a good fluid indicator. This is because Mu-Rho is largely influenced by the S-wave, which is not affected by fluid type (Ogbamikhumi, & Igbinigie, 2020).

The cross-plot of Poisson Ratio against P-Impedance is also able to discriminate fluid type within a rock (figure 6). While P-Impedance is not a good lithology indicator, the property records a much higher value for water-bearing sands compared to hydrocarbon-bearing sands. Likewise, the Poisson Ratio also records the same trend, though the difference between the two-fluid type is relatively smaller. However, when cross-plotted together, a clear separation between water-bearing sands and hydrocarbon-bearing sands could be established.

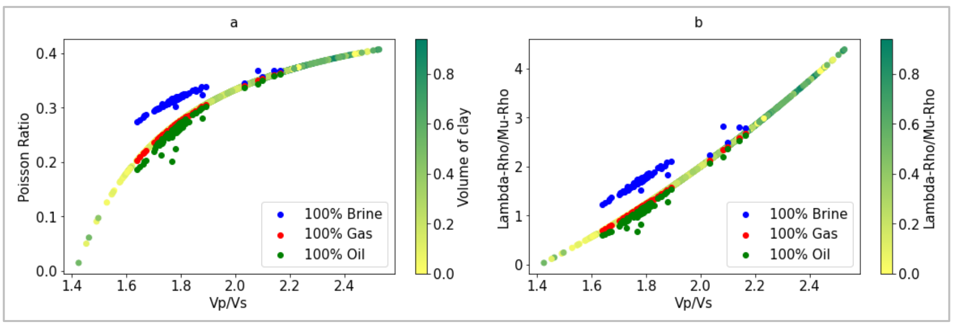

Fig. 6. Cross-plots of a) Poisson-Ratio vs Vp/Vs, and b) Lambda-Rho/Mu-Rhos vs Vp/Vs for actual well data and fluid substitution scenarios.

The Poisson Ratio vs Vp/Vs and Lambda-Rho/Mu-Rho vs Vp/Vs cross-plot are not just great lithology indicators but are also excellent in discriminating between water-bearing and hydrocarbon-filled reservoirs. This is because the water-bearing reservoirs records a much greater Poisson Ratio and Lambda-Rho/Mu-Rho value compared to the hydrocarbon-bearing reservoirs.

While the parameters in the above cross-plots can discriminate between brine and hydrocarbon-filled sands, most of them are not as sensitive to differentiate between oil and gas. Instead, the following cross-plots are the most sensitive in differentiating between oil and gas at 100% saturation, though overlaps still exist.

The parameters that are most sensitive to 100% Gas and 100% Oil saturation are Vp, Density and Bulk Modulus. In the Vp vs Bulk Modulus cross-plot, the gas-bearing sand records a higher Bulk Modulus and Vp value compared to the oil-bearing sands (figure 7). In the Vp vs Density cross-plot, the gas bearing sand records a lower density but higher Vp value compared to the oil-bearing sand. In the Density vs Bulk Modulus cross-plot, the gas-bearing sands records a higher Bulk Modulus but lower density value. The unique ranges of oil and gas bearing sands for the three parameters causes these three cross-plots to be able to distinguish between the oil and gas bearing reservoirs. However, in real reservoir conditions, hydrocarbon saturation is rarely at 100%. A lower hydrocarbon saturation scenario may result in more overlap between the oil and gas plots.

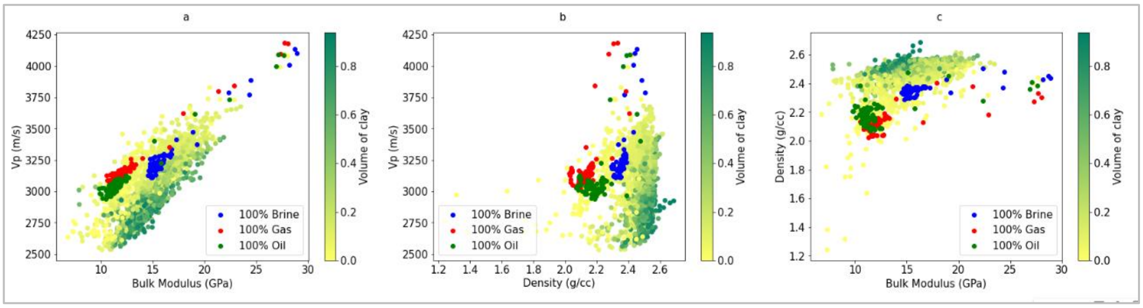

Fig. 7. Cross-plots of a) Vp vs Bulk Modulus, b) Vp vs Density and c) Density vs Bulk Modulus for actual well data and fluid substitution scenarios.

4. Conclusion

The sensitivity of elastic properties towards different lithology and fluid for Well X in Malay Basin is presented and discussed in detail. The Poisson Ratio and Lambda-Rho/Mu-Rho properties are the most sensitive to lithology changes, specifically in differentiating between sand and shale. The Shear Impedance, Shear Modulus, Young Modulus and Mu-Rho are also good indications of lithology. The Lambda-Rho, Lambda-Rho/Mu-Rhos, P-Impedance and Poisson Ratio properties are the most sensitive to fluid changes, especially in discriminating between oil and gas. The elastic parameters that are most sensitive towards hydrocarbon type at 100% saturation are the Vp, Density and Bulk Modulus. Analysis of the result confirms that the sand in Well X is hydrocarbon bearing. The identified elastic parameters that are sensitive to lithology and fluid fill could be used for future seismic-based inversion in the field and its surrounding. The developed Python code for Gassman fluid substitution and elastic properties calculation and cross-plot is also beneficial for geologist to conduct a quick-look analysis on the prospectivity of their exploration area.

Acknowledgements

The authors thank Petronas Carigali Sdn. Bhd. (PCSB) and Universiti Teknologi PETRONAS (UTP) for providing the data used for this study.

References

Lubis, L. A., Ghosh, D. P., & Hermana, M. (2016). Elastic and electrical properties evaluation of low resistivity pays in Malay Basin clastic reservoirs. *IOP Conf. Series: Earth and Environmental Science, 38*(1), 012004. DOI: 10.1088/1755-1315/38/1/012004.

Kumar, D. (2006). A tutorial on Gassmann Fluid Substitution: Formulation, algorithm and Matlab Code. *Geohorizons*, 4-12.

Bodunde, S. S., & Enikanselu, P. A. (2018). Integration of 3-D seismic and petrophysical analysis with rock physics analysis in the characetrization of SOKAB field, Niger delta, Nigeria. *Journal of Petroleum Exploration and Production Technology*, 9, 899-909.

Smith, T. M., Sondergald, C. H., & Rai, C. S. (2003). Gassmann fluid substitutions: a tutorial. *Geophysics*, 68(2), 430-440. https://doi.org/10.1190/1.1567211 .

Huang, L., Stewart, R. R., Sil, S. & Dyaur, N. (2014). Fluid substittuion effects on seismic anisotropy. *Journal of Geophysical Research: Solid Earth*, 120, 850-863. https://doi.org/10.1002/2014JB011246 .

Ogbamikhumi, A. & Igbinigie, N. S. (2020). Rock physics attribute analysis for hydrocarbon prospectivity in the Eva field onshore Niger Delta Basin. *Journal of Petroleum Exploration and Production Technology*, 10(2020), 3127-3138. https://doi.org/10.1007/s13202-020-00975-5

Abbey, P. C., Okpogo, E. U. & Atueyi, I. O, (2017). Application of rock physics parameters for lithology and fluid prediction of 'TN' field of Niger Delta basin, Nigeria. *Egyptian Journal of Petroleum*, 27(2018), 853-866. https://doi.org/10.1016/j.ejpe.2018.01.001 .

Appendix A. Phyton Codes

The followings are the Python codes for the calculations conducted in this research.

A.1. Python coding for elastic properties calculation

```
import pandas as pd
import matplotlib.pyplot as plt
import warnings
warnings.filterwarnings('ignore')
data = pd.read_csv('/content/drive/MyDrive/Colab Notebooks/project/Well_msc.csv')
well = data.rename(columns={'Depth (ms)': 'DEPTH',
                  'GR[API]': 'GR',
                  'Rt[ohm.m]': 'RT',
                  'Rho[g/cc]': 'RHOB',
                  'Vp[m/s]': 'VP',
                  'Vs[m/s]': 'VS',
                  'Sw':'SW',
                  'Por':'PHI',
                  'Vclay':'Vclay'
                  })

#Calculation of elastic properties
DEN_gcc=(well.iloc[:,3]) #g/cc
DEN_kgm=(well.iloc[:,3])*1000 #kg/m3
VP_ms=well.iloc[:,4] #m/s
VS_ms=well.iloc[:,5] #m/s

#use density with g/cc
well['SI'] = DEN_gcc*(VS_ms) #shear impedence (g/cc * m/s)
well['AI'] = DEN_gcc*(VP_ms) #acoustic impedence (g/cc * m/s)
well['Pratio'] = ((VP_ms**2)-(2*(VS_ms**2)))/(2*(VP_ms**2-VS_ms**2)) # poisson's ratio (unitless)


well['LR'] = ((well['AI']**2) - (2*((DEN_gcc*VS_ms)**2)))/(10**6) # Lambda Rho (GPa*g/cc)
well['MR'] = ((VS_ms*DEN_gcc)**2)/(10**6) # Mu Rho (GPa*g/cc)

#use density with Kg/m3
well['E'] = (((DEN_kgm*(VS_ms**2))*((3*(VP_ms**2)) - (4*(VS_ms**2))))/((VP_ms**2) - (VS_ms**2)))/(10**9) #Young's modulus (GPa)
well['BulkModulus']=(DEN_kgm*((VP_ms**2)-((4/3)*(VS_ms**2))))/(10**9) #bulk modulus (GPa)
well['shear modulus']=(DEN_kgm*(VS_ms**2))/(10**9) #shear modulus (GPa)

well['Vp/Vs']=VP_ms/VS_ms #unitless
well['LR/MR']=(well['LR']/well['MR']) #unitless

well.describe()
```

A.2. Python coding for fluid substitution calculation

```
WI = well[(well.DEPTH >= 1670 ) & (well.DEPTH <= 1683)] # Working interval

def gassman(df,model_fluid,modeled_Sw):
  import numpy as np
  den_init = df['RHOB']  #* 1000 #convert g/cm3 to kg/m3
  Vp_init = df['VP'] #* 3.6 # convert from km/h to m/s
  Vs_init = df['VS'] #* 3.6 # convert from km/h to m/s
  Init_sw = df['SW']
  Vol_clay = df['Vclay']
  Por = df['PHI']

  K_init = (den_init*1000*((Vp_init**2)-((4/3)*(Vs_init**2))))*(10**(-9)) #gpa
  G_init = (den_init*1000*(Vs_init**2))*(10**(-9))  #mu

  kwtr = 2.29 # GPa

  if model_fluid == 'gas':
    KF_2 = 0.0021 # GPa
    Dens_2 = 0.1 #g/cc
  elif model_fluid == 'oil':
    KF_2 =  1 # Oil GPa
    Dens_2 = 0.75

  Kf_init = ((Init_sw/kwtr)+((1-Init_sw)/KF_2))**(-1) #kf_init

  K_q = 37 # Quartz (in GPa)
  K_c = 22 # Clay (in GPa)
  F_q = 1-Vol_clay

  K_v = (F_q*K_q) + (Vol_clay*K_c) # kvoigt
  K_r = ((F_q/K_q) + (Vol_clay/K_c))**(-1) # kreuss
  K_h = (K_v + K_r)/2 #kvoigt-russ-hill
  K_min = K_h #k mineral

  # Step 4: Calculate Kf
  Kf_final = ((modeled_Sw/kwtr)+((1-modeled_Sw)/KF_2))**(-1) #kreuss

  # step 5: Calculate Bulk Modulus of fluid at Final Condition
  K_dry_init = (K_init/(K_min-K_init)) - (Kf_init/(Por*(K_min-Kf_init)))

  # step 6.a: Calculate K_dry at Initial Condition
  K_final_p1 = K_dry_init + (Kf_final/(Por*(K_min-Kf_final)))
  K_final = (K_final_p1*K_min)/(1+K_final_p1)

  # step 6.b: Calculate K_dry at Initial Condition
  G_final = G_init

  # step 7: Calculate K_dry at Initial Condition
  Dens_oil = 0.2 # Density of Hydrocarbon
  Dens_w =1 # Density of Water
  Dens_q = 2.65 #Density of Quartz
  Dens_c = 2.2 #Density of Clay

  Dens_f_1 = (Init_sw * Dens_w) + ((1-Init_sw)*Dens_2)
  Dens_f_2 = (modeled_Sw * Dens_w) + ((1-modeled_Sw)*Dens_2)
  Dens_f_final = den_init + (Por*(Dens_f_2 - Dens_f_1)) # Bulk density of saturated rock

  # step 7a: Calculate K_dry at Initial Condition
  Final_vp = np.sqrt(((K_final + ((4/3)*G_final))*(10**9))/(Dens_f_final*(10**3))) # m/s
  Final_vs = np.sqrt((G_final*(10**(9)))/(Dens_f_final*(10**3)))

  depth = df['DEPTH']

  import matplotlib.pyplot as plt
  plt.figure(figsize=(15,5))
  plt.subplot(131)
  plt.plot(Final_vp,depth,'r',label='Vp FRM')
  plt.plot(Vp_init,depth,'k',label='Vp original')
  plt.gca().invert_yaxis()
  plt.title('Vp (m/s')
  plt.legend(loc='lower right')

  plt.subplot(132)
  plt.plot(Final_vs,depth,'r',label='Vs FRM')
  plt.plot(Vs_init,depth,'k',label='Vs original')
  plt.gca().invert_yaxis()
  plt.title('Vs (m/s')
  plt.legend(loc='lower right')

  plt.subplot(133)
  plt.plot(Dens_f_final,depth,'r',label='RHOB FRM')
  plt.plot(den_init,depth,'k',label='RHOB original')
  plt.gca().invert_yaxis()
```